Electron mass stopping power in H_2

Dmitry V. Fursa,[1] Mark C. Zammit,[1,2] Robert L. Threlfall,[1] Jeremy S. Savage,[1] and Igor Bray[1]
[1]*Curtin Institute for Computation and Department of Physics, Astronomy and Medical Radiation Sciences, Curtin University, Perth, Western Australia 6102, Australia*
[2]*Theoretical Division, Los Alamos National Laboratory, Los Alamos, New Mexico 87545, USA*
(Received 28 April 2017; revised manuscript received 7 July 2017; published 23 August 2017)

Calculations of electron mass stopping power (SP) of electrons in H_2 have been performed using the convergent close-coupling method for incident electron energies up to 2000 eV. Convergence of the calculated SP has been established by increasing the size of the close-coupling expansion from 9 to 491 states. Good agreement was found with the SP measurements of Munoz *et al.* [Chem. Phys. Lett. **433**, 253 (2007)].

DOI: 10.1103/PhysRevA.96.022709

I. INTRODUCTION

Interaction of high-energy particles (x-rays, protons, and ions) with matter leads to the production of a large number of secondary electrons. It is well established that the secondary electrons play an important role in DNA damage [1,2]. Assessment and modeling of radiation damage, therefore, requires accurate account of the secondary electron interactions with atoms and molecules. Furthermore, electron impact processes play an important role in studies of planetary atmospheres [3], interstellar medium [4], fusion, and industrial plasmas [5]. Given the large number of reaction channels involved in such processes, theoretical techniques are viewed as the most appropriate to obtain the required collision data, while experiment provides crucial tests for theoretical models. For electron-atom collisions present-day advanced theoretical methods [6–8] can provide detailed results for electron scattering cross sections for many atoms to high accuracy. The situation is different for electron-molecule collisions where reaction channels leading to molecular vibrations, rotations, and dissociation present additional challenges and progress was largely limited to low-energy scattering [9,10].

In this paper we are interested in the electron mass stopping power (SP) for molecular hydrogen. The SP (or energy loss function) is an important parameter of interest in medical research [11,12], environmental and technological applications [13,14] where energy deposition of electrons is of primary importance. The H_2 SP is of special interest in astrophysics [4,15–17] as molecular hydrogen is the most abundant molecule in the universe, particularly in the interstellar space and in the atmospheres of gas giants and the outermost planets of the solar system.

The calculations of the SP have been performed for a number of molecules using the Bethe formula [18–20] combined with the Bragg's additivity rule [21] with results available, for example, from the NIST database [22] above 1000 eV. The Bethe formula is expected to be accurate at high incident electron energies (>1000 eV). An extension of the Bethe formula to low and intermediate energies has been attempted in a number of studies using the concepts of target effective atomic number and mean excitation energy [23–25]. However, an accurate evaluation of the SP in molecules at energies below 1000 eV requires a complete set of electron impact cross sections for all important reaction channels including excitation, ionization and dissociation. A number of studies have used a compilation of cross sections for molecular hydrogen to estimate the SP [17,26,27]. Such collision data sets were based on the experiment available at the time, semiempirical ionization cross sections, and the Born-Bethe excitation cross-section results extended to low energies by phenomenological techniques.

Experimental determination of the electron SP in molecular hydrogen have been conducted by Munoz *et al.* [28] in the energy range 15–5000 eV. In the experiment the measurement of the energy loss spectra have been used to determine the mean excitation energy. The latter was combined with the total inelastic cross sections (obtained from available total and elastic cross sections) to obtain an estimate of the SP. At energies above 1000 eV reasonable agreement (within 20%) was found with the NIST molecular hydrogen results calculated with the Born-Bethe theory [22], where the NIST data were the only results used for comparison. Given the observed discrepancy between the experiment and Born-Bethe results for the electron SP in methane [29] and total cross sections for a number of diatomic molecules [30,31], a fresh look at the calculations of total cross sections and SP at intermediate and high energies is highly desirable.

Molecular hydrogen is the simplest neutral molecule and is a natural starting point for application of advanced theoretical techniques to SP calculations in molecules. We have recently obtained a comprehensive set of electron-impact elastic, excitation, ionization, and total cross sections for e^--H_2 scattering over a wide energy range (0.1–300 eV) [32,33] using the convergent close-coupling (CCC) method. Here we extend the CCC calculations to higher energies (2000 eV) where comparison with the Born-Bethe theory results is possible. These cross sections allow the modeling of various processes related to the interaction of electrons with H_2 molecules, and in particular to evaluate the SP and mean excitation energy. We, therefore, are in position to examine the robustness of the experimental approach for determining the SP, verify the accuracy of the approximate techniques utilized in previous studies, and provide the first fully *ab initio* calculations of the SP for low and intermediate incident electron energies.

Previously we have applied the CCC method to study antiproton stopping power for a number of atomic targets [34], hydrogen, and water molecules [35]. Here we extend stopping power calculations to light (electron) projectiles. The paper is organized as follows. In the next section we describe the CCC method and SP calculations for e^--H_2 collisions. Results and discussion are given in Sec. III and conclusions are formulated in Sec. IV.

 ©2017 American Physical Society

II. THEORETICAL METHOD

Application of the CCC method to electron scattering from molecular hydrogen has been discussed in detail in Refs. [32,33,36]. Only a brief overview is presented here.

A. CCC method

The molecular CCC method [37] is formulated in a single-center coordinate system and utilizes the Born-Oppenheimer approximation of the scattering wave function. All calculations are performed in the fixed-nuclei approximation. The internuclear distance R is chosen to be the average internuclear distance of the H_2 ground state, $R = 1.448\ a_0$. Due to the separation of the electronic and nuclei degrees of freedom the problem reduces to the solution for electronic wave functions only. The body frame with the z axis aligned along the internuclear line and the origin at the midpoint between the two nuclei of H_2 has been used to obtain the electronic target wave functions. These will be used to form a close-coupling expansion of the total electronic scattering wave function. For the brevity of notation we suppress the explicit dependence on R in all formulas.

Molecular electronic target states $\Phi_n^N(x_1,x_2)$ are constructed via a diagonalization procedure of the electronic Hamiltonian H_T in a basis constructed from appropriately symmetry-adapted two-electron configurations for each set of terms of the conserved quantum numbers (m_t,π_t,s_t), where m_t is the total target angular momentum projection, s_t is the spin, and π_t is the parity:

$$\Phi_n^N(x_1,x_2) = \sum_{\alpha\beta} C_{\alpha\beta}^{(n)} \phi_\alpha(\boldsymbol{r}_1)\phi_\beta(\boldsymbol{r}_2) X(s_n,v_n), \tag{1}$$

where the 1 and 2 indices are used for the target space, x is used to denote both the spatial and spin coordinates, and the two-electron spin function is given by

$$X(s,v) = \sum_{m_1 m_2} C^{sv}_{\frac{1}{2}m_1\frac{1}{2}m_2} \chi_{m_1}(\sigma_1)\chi_{m_2}(\sigma_2), \tag{2}$$

and $C^{lm}_{l_1m_1l_2m_2}$ is a Clebsch-Gordon coefficient.

The one-electron functions in Eq. (1) are characterized by the orbital angular momentum projection m_α and parity $\pi_\alpha = (-1)^{l_\alpha}$, and expressed as

$$\phi_\alpha(\boldsymbol{r}) = \frac{1}{r}\varphi_{k_\alpha l_\alpha}(r) Y_{l_\alpha m_\alpha}(\hat{\boldsymbol{r}}), \tag{3}$$

where the radial part is taken as the Laguerre basis functions,

$$\varphi_{kl}(r) = \sqrt{\frac{\alpha_l (k-1)!}{(k+l)(k+2l)!}} (2\alpha_l r)^{l+1} e^{-\alpha_l r} L_{k-1}^{2l+1}(2\alpha_l r). \tag{4}$$

Here α_l are the exponential falloff parameters, L_{k-1}^{2l+1} are the associated Laguerre polynomials and k ranges from 1 to N_l, the number of functions for a given value of l.

The resulting set of target (pseudo)states $\{\Phi_n^N\}$, $n = 1,\ldots,N$ satisfy

$$\langle \Phi_{n'}^N | H_T | \Phi_n^N \rangle = \varepsilon_n^N \delta_{n'n}, \tag{5}$$

where ε_n^N is the energy of the state Φ_n^N.

These target states are used to perform a multichannel expansion of the total electronic scattering wave function

$$\Psi_i^{N(+)}(x_0,x_1,x_2) = \mathcal{A}\psi_i^{N(+)}(x_0,x_1,x_2) = \mathcal{A}\sum_{n=1}^{N} f_n^{N(+)}(x_0)\Phi_n^N(x_1,x_2), \tag{6}$$

where the 0 index is used to denote the projectile space and (+) denotes outgoing spherical wave boundary conditions. The antisymmetrization operator is $\mathcal{A} = 1 - P_{01} - P_{02}$ and P_{0i} is the space exchange operator.

The total electronic wave function is a solution of the Schrödinger equation

$$(E^{(+)} - H)\Psi_i^{N(+)} = 0, \tag{7}$$

where $H = K_0 + V + H_T$ is the total (electronic) Hamiltonian of the scattering system, K_0 is the projectile electron kinetic energy operator and V is the projectile-target interaction potential. Substitution of the expansion (6) into the Schrödinger equation leads to a set of momentum-space Lippmann-Schwinger close-coupling equations for the T matrix

$$\langle \boldsymbol{k}_f^{(-)}\Phi_f^N | T^N | \Phi_i^N \boldsymbol{k}_i^{(+)} \rangle = \langle \boldsymbol{k}_f^{(-)}\Phi_f^N | V | \psi_i^{N(+)} \rangle, \tag{8}$$

where $|\boldsymbol{k}^{(\pm)}\rangle$ is a projectile electron distorted wave with energy $\epsilon_k = k^2/2$.

Expanding the projectile wave function in partial waves

$$|\boldsymbol{k}^{(\pm)}\rangle = \frac{1}{k}\sum_{L,M} i^L e^{\pm i\delta_L} Y_{LM}^*(\hat{\boldsymbol{k}})|kL\rangle, \tag{9}$$

where δ_L is the distorting phase shift and the sum is taken to some maximum value of $L_{\max}$, allows formulation of a set of close-coupling equations for the partial-wave T matrix. These equations are written separately for each total symmetry $(\mathcal{M},\Pi,\mathcal{S})$ specified by the total angular momentum projection $\mathcal{M}$, parity Π, and spin $\mathcal{S}$,

$$T^{\mathcal{M}\Pi\mathcal{S}}_{fL_fM_f,iL_iM_i}(k_f,k_i) = V^{\mathcal{M}\Pi\mathcal{S}}_{fL_fM_f,iL_iM_i}(k_f,k_i) + \sum_{n=1}^{N}\sum_{L'M'}\sum\!\!\!\!\!\!\int_k dk \times \frac{V^{\mathcal{M}\Pi\mathcal{S}}_{fL_fM_f,nL'M'}(k_f,k) T^{\mathcal{M}\Pi\mathcal{S}}_{nL'M',iL_iM_i}(k,k_i)}{E^{(+)} - \varepsilon_k - \varepsilon_n^N + i0}, \tag{10}$$

and are solved by standard techniques [36,38].

The projectile-target interaction potential V is not spherically symmetric and results in the coupling of partial-wave T-matrix elements with different values of the projectile angular momentum L. As the size of the projectile partial-wave expansion (9) increases the size of the close-coupling equations (10) grows dramatically. This is also the case when the number of target states used in the close-coupling expansion (6) is increased. The principal problem of applying the close-coupling method to electron-molecule scattering is demonstrating convergence in the cross sections with increasing size of the partial wave and close-coupling expansions.

Comparison with experiment requires transformation of the body-frame T matrix to the laboratory frame, which is done utilizing an appropriate orientation averaging of the

cross sections [36]. The resulting partial-wave integrated cross sections (ICS) for a transition from an initial state i to the final state f are given by

$$\sigma_{f,i}^{\mathcal{M}\Pi\mathcal{S}} = \frac{k_f}{k_i}\frac{1}{4\pi}\sum_{\substack{L_f,L_i\\M_f,M_i}} \left|F_{fL_fM_f,iL_iM_i}^{\mathcal{M}\Pi\mathcal{S}}\right|^2, \tag{11}$$

where

$$F_{fL_fM_f,iL_iM_i}^{\mathcal{M}\Pi\mathcal{S}} = -(2\pi)^2(k_fk_i)^{-1}i^{L_i-L_f} \times T_{fL_fM_f,iL_iM_i}^{\mathcal{M}\Pi\mathcal{S}}(k_f,k_i). \tag{12}$$

Note that for elastic scattering the physical T matrix is extracted from the distorted-wave T matrix [36]. The spin-averaged cross section summed over partial waves is given by

$$\sigma_{fi} = \sum_{\mathcal{S}}\frac{2\mathcal{S}+1}{2(2s_i+1)}\sum_{\mathcal{M}\Pi}\sigma_{fi}^{\mathcal{M}\Pi\mathcal{S}}. \tag{13}$$

Convergence of the excitation cross sections with respect to the partial-wave expansion can be improved by using the Born top-up or analytical Born subtraction procedure. This method relies on the fact that for large partial waves the excitation T matrix is well approximated by the first term on the right-hand side of the Lippmann-Schwinger equation (10). The excitation cross sections are then obtained as

$$\sigma_{fi}^{\mathcal{S}} = \sum_{\mathcal{M}\Pi}\left(\sigma_{fi}^{\mathcal{M}\Pi\mathcal{S}} - \sigma_{fi}^{\mathcal{M}\Pi}\right) + \sigma_{fi}^{\mathrm{AB}}, \tag{14}$$

where $\sigma_{fi}^{\mathrm{AB}}$ and $\sigma_{fi}^{M\Pi}$ are the orientation averaged analytical and partial-wave Born ICS [37]. In the present calculations the maximum total angular momentum projection and the maximum projectile angular momentum are chosen to be the same, and $\mathcal{M}_{\max} = L_{\max} = 8$ proved to be sufficient to provide convergent results by comparison with also conducted calculations with $\mathcal{M}_{\max} = L_{\max} = 6$.

The use of Sturmian (Laguerre) functions as the underlying one-electron basis allows us to model both the bound and continuum spectra of the target by a finite-size expansion in the set of states $\{\Phi_n^N\}$. As the size N of the expansion increases these states provide an accurate representation of the low-lying bound states of the target and an increasingly dense square-integrable representation of the target continuum, which allows the CCC method to model all possible electronically driven reaction channels including ionization. Such an approach has been extensively used in electron-atom scattering [6,39], while conversely in electron-molecule scattering, such an approach has only been applied to a limited number of problems [33,37,40,41]. For e^--H_2 scattering the previous most detailed results have been obtained with the close-coupling expansion comprising the seven lowest nondegenerate states [42–44]. We have shown already that such a small expansion is insufficient to accurately model e^--H_2 excitation processes [33], here we demonstrate this for the SP.

B. Calculation details

To establish convergence of the close-coupling expansion we have performed calculations in a number of models by increasing the size of the calculations from 9 to 491 states, with degenerate states $m_t = \pm|m_t|$ counted separately. We use the acronym "CC" for models that include only bound states and "CCC" for those that also include pseudostates modeling ionization channels. The largest CCC(491) model was obtained with an underlying Laguerre basis constructed from $N_l = 17 - l$ functions for $l \leqslant 3$. This model has 491 states and includes 92 bound states of H_2 plus 399 continuum pseudostates with energies up to 1000 eV. Comparison with the result obtained with the CC(92) model, that includes only the 92 bound states, allows us to determine the importance of the ionization channels. We have performed two other calculations that have a smaller underlying Laguerre basis with $N_l = 15 - l$ functions. The larger of the two models CCC(427), included functions with $l \leqslant 3$, while the CCC(259) model included functions with $l \leqslant 2$. The calculation in the CCC(259) model has been performed with the projectile partial wave expansion $\mathcal{M}_{\max} = L_{\max} = 6$ to verify the convergence with respect to the partial wave expansion.

A good agreement between the two largest models, CCC(491) and CCC(427), would indicate the convergence of the obtained collision data with respect to the discretization of the target continuum. Comparison with the CCC(259) model gives an indication of the convergence with respect to including target states constructed from orbitals with larger angular momentum l. Due to the unitarity of the close-coupling method the convergence with the underlying Laguerre basis orbital angular momentum l is fast [45]. The states with the largest orbital angular momentum values for a given structure model have cross sections that are somewhat too large as they model excitation to states with higher l values (not included in the expansion), however, the cross sections summed over all states are particularly rapidly convergent. Finally, we also present results obtained with the first nine states of H_2. Comparison between the results of the CC(92) and CC(9) models will indicate the importance of the high-lying bound states in the SP calculations.

The CCC calculations reported in Refs. [32,33] have been conducted up to 300 eV. Here we extend the CCC(491) model to 700 eV. The exchange interaction between the projectile and target electrons and interchannel coupling become progressively less important as the incident electron energy increases. For energies above 500 eV we have conducted calculations with the CCC(491) model neglecting exchange and retaining only singlet states. The collision cross sections have also been obtained using the first Born approximation (FBA) to determine the incident electron energy for which interchannel coupling becomes negligible.

C. Stopping power

Here we use the results of the CCC calculations to obtain the SP, or energy loss per unit path length, of electrons in H_2 using the following relation

$$-\frac{1}{\rho}\frac{dE}{dx} \equiv Q_{\mathrm{SP}} = \frac{N_a}{M}\sigma_{\mathrm{sp}}, \tag{15}$$

where N_a is the Avogadro number, ρ is the density of the target, and M is the molar mass. Following our previous work [34], the stopping cross section in the CCC method can be

obtained as

$$\sigma_{\rm sp} = \sum_{n=1}^{N_T} (\varepsilon_n - \varepsilon_0)\sigma_n, \tag{16}$$

where σ_n is the electron impact excitation cross section from the ground state (indexed $n = 0$) of H_2 with energy ε_0 to a final state n with energy ε_n at an incident electron energy E_i. For clarity of presentation, we have dropped an explicit dependence on the incident electron energy E_i in all equations. The sum in Eq. (16) goes over all N_T open (energy accessible) target states in the close-coupling expansion including positive energy pseudostates. Retaining in the sum on the right-hand side of Eq. (16) only the negative energy pseudostates (relative to the H_2^+ ground state at $R = 1.448\ a_0$) we can obtain an estimate of the SP due to the bound spectrum of H_2 while including only the positive energy pseudostates allows us to determine the SP due to the ionization channels.

To facilitate comparison with the experiment [28] and Born-Bethe calculations [22] it is useful to define a mean excitation energy

$$\bar{E} = \frac{\sigma_{\rm sp}}{\sigma_{\rm inel}}, \tag{17}$$

where the total inelastic (reaction) cross section is given by

$$\sigma_{\rm inel} = \sum_{n=1}^{N_T} \sigma_n, \tag{18}$$

and is equal to the difference between the total $\sigma_{\rm tot}$ and elastic $\sigma_{\rm el}$ scattering cross sections. The SP (15) can now be written as

$$-\frac{1}{\rho}\frac{dE}{dx} = \frac{N_a}{M}\bar{E}\sigma_{\rm inel} = \frac{N_a}{M}\bar{E}(1-\eta)\sigma_{\rm tot}, \tag{19}$$

where $\eta = \sigma_{\rm el}/\sigma_{\rm tot}$. This form of the electron mass SP (19) is consistent with the analysis of Munoz *et al.* [28]. They determined the mean excitation energy $\bar{E}$ from their measured energy-loss spectrum, and obtained the total inelastic cross sections (18) from recommended total scattering cross sections and the values of parameter η obtained from fitting to the data of van Wingerden *et al.* [46]. Note, however, that while Eq. (19) offers a useful alternative for the experimental evaluation of the SP, in the present calculations both Eqs. (15) and (19) necessarily produce the same values of the SP.

The SP calculated in this work refer to the electronic excitations of H_2. Within the fixed-nuclei approximation adopted in the present CCC calculations we neglect an explicit account of vibrational and rotational excitations. Explicit account of rovibrational excitations is of importance only at very low energies, well below the first excitation threshold, and will be considered elsewhere. The dissociative processes are accounted for indirectly in the present technique, as in the fixed-nuclei approximation the calculated excitation cross sections describe scattering to all rovibrational levels of electronic excited states, including dissociation.

III. RESULTS AND DISCUSSION

We present convergence studies for the electron mass SP in Fig. 1. We find very good agreement between CCC(491), CCC(427), and CCC(259) results that establishes the convergence of our calculations with an accuracy of better than 5%. At high energies, 500 eV and above, the no-exchange approximation becomes sufficiently accurate. From 1000 eV the FBA becomes valid and is in good agreement with the Born-Bethe results [22]. The CC(92) model significantly underestimates the SP at energies larger than 30 eV. This demonstrates the importance of the ionization channels for SP calculations. Comparison between the CC(92) and CC(9) models shows the importance of excitations to the highly excited bound states.

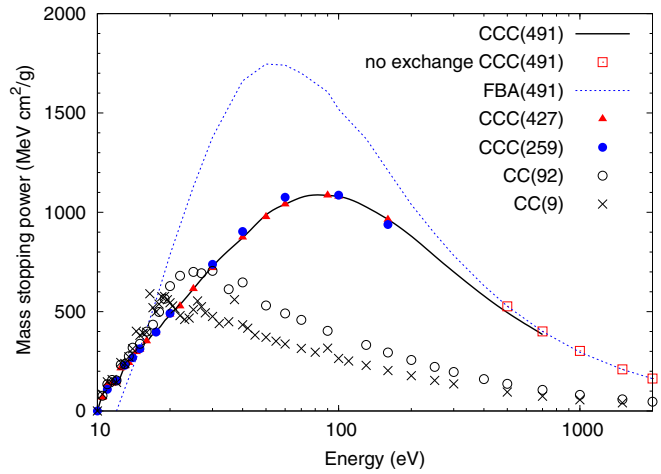

FIG. 1. Convergence studies of the mass stopping power for electron scattering on the ground state of H_2. CCC and CC models are described in the text.

The results of the CCC(491) model have been combined at high energies with no-exchange CCC(491) and FBA results. These combined data, labeled as CCC are presented in Table I and Fig. 2 together with its partition on the bound and ionization components. In Fig. 3 the CCC results

TABLE I. Mass stopping power (SP) in units of MeV cm^2/g and mean excitation energy ($\bar{E}$) in units of eV for electron (of incident energy E_i) scattering on the ground state of H_2 calculated using the CCC method.

E_i (eV)	SP	$\bar{E}$	E_i (eV)	SP	$\bar{E}$
11	135.6	10.3	50	987.0	17.5
12	134.1	10.3	60	1040.6	18.1
13	228.1	11.3	70	1075.0	18.7
14	268.8	11.5	90	1085.0	19.5
15	321.7	11.9	100	1079.7	19.8
16	346.8	12.3	130	1027.0	20.6
17	388.5	12.7	160	964.2	21.2
18	416.3	13.0	200	880.0	21.8
19	453.9	13.3	250	780.1	22.1
20	482.4	13.6	300	700.0	22.3
22	527.4	14.0	500	495.7	22.8
25	614.5	14.7	700	384.8	22.9
30	727.6	15.6	1000	294.0	23.1
35	808.5	16.1	1500	208.5	22.9
40	871.7	16.6	2000	162.7	22.7

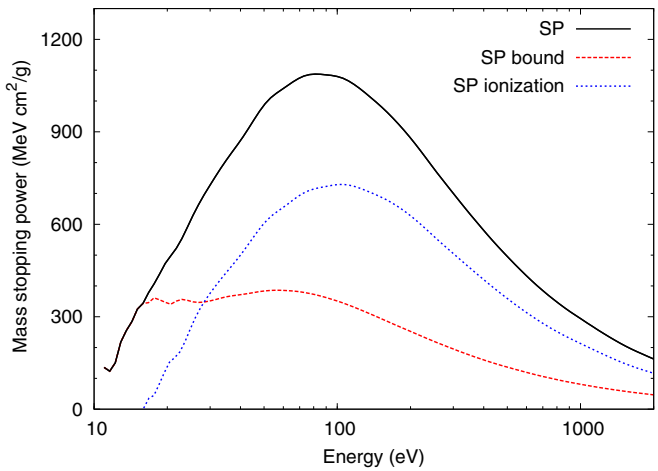

FIG. 2. The bound and ionization components the mass stopping power (SP) for electron scattering on the ground state of H_2 calculated using the CCC method.

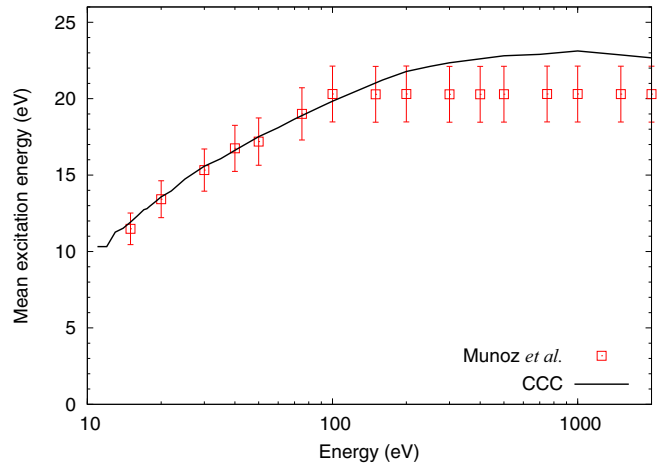

FIG. 4. Mean excitation energy $\bar{E}$ for electron scattering on the ground state of H_2. The CCC results are described in the text. Experimental data are due to Munoz *et al.* [28].

are compared with the estimates of the SP obtained by Gumus [25], Takayanagi and Nakata [26], Miles *et al.* [27], and Dalgarno *et al.* [17] and the experiment of Munoz *et al.* [28]. Previous estimates of the SP were based on the phenomenological extension of the Bethe formula to low and intermediate energies [25] and evaluation of the available experimental and theoretical data for excitation and ionization cross sections [17,26,27]. These studies utilized theoretical results that were predominately based on Born-Bethe theory with phenomenological modifications at low energies. Given the large (>20%) uncertainties of the experimental e^--H_2 excitation cross sections and difficulty in producing reliable cross sections from Born-Bethe theory at low energies the uncertainties in these SP estimates are expected to be large. This is clearly seen in Fig. 3 where the differences between the previous SP estimates are particularly large below 100 eV.

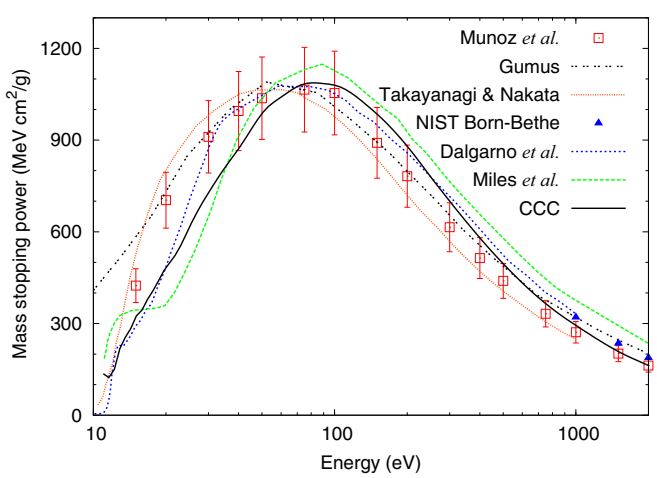

FIG. 3. Mass stopping power for electron scattering on the ground state of H_2. The CCC results are described in the text. Experimental data are due to Munoz *et al.* [28]. The estimates of the SP are due to Gumus [25], Takayanagi and Nakata [26], Miles *et al.* [27], Dalgarno *et al.* [17], and the Born-Bethe results are from the NIST database [22].

The CCC results agree best with the estimate of Dalgarno *et al.* [17]. The CCC results, the previous estimates of Dalgarno *et al.* [17], Gumus [25], Takayanagi and Nakata [26], Miles *et al.* [27], and the experiment [28] show the maximum value for SP at around 75 eV, which is a similar position to the maximum for methane-based tissue equivalent gas mixture [29]. The experiment of Munoz *et al.* [28] has uncertainty of 13%. We find that the CCC results are somewhat below the experiment for incident electron energies less than 50 eV, but in good agreement at higher energies. The disagreement below 50 eV is rather unexpected and deserves some attention.

It is important to emphasize that Munoz *et al.* [28] have not measured the SP directly. They derived the mean excitation energy from the measured energy loss spectra and used it to estimate the experimental SP via Eq. (19). This procedure required an estimate of the total and elastic cross sections that come with their own uncertainties. It is, therefore, preferable to compare directly with the quantity being measured. We extracted the mean excitation energy values from the data presented by Munoz *et al.* [28] and assigned 9% uncertainty to the experimental values, the same as the uncertainty reported at 100 eV. The results of the CCC calculations for $\bar{E}$ are given in Table I and are compared with the experiment in Fig. 4. We find very good agreement with our calculations from the lowest measured energy point at 15 eV up to 300 eV. At larger energies our values are about 10% higher than the experiment and are just above the experimental error bars. The measured mean excitation energy remains approximately constant above 100 eV with the value of 20.3 ± 1.8 eV [28]. Our results show a similar behavior but the constant value of 23 eV at energies larger than 400 eV.

The mean excitation energy enters as a parameter in the Born-Bethe procedure for the determination of the SP. The value of 19.2 eV was adopted in the Born-Bethe method [22] and is calculated from the oscillator strength distribution. Similar calculations using the oscillator strengths obtained in the CCC(491) model give the value of 20.9 eV in the length form and 19.4 eV in the velocity form. The difference between the length and velocity forms gives an indication of

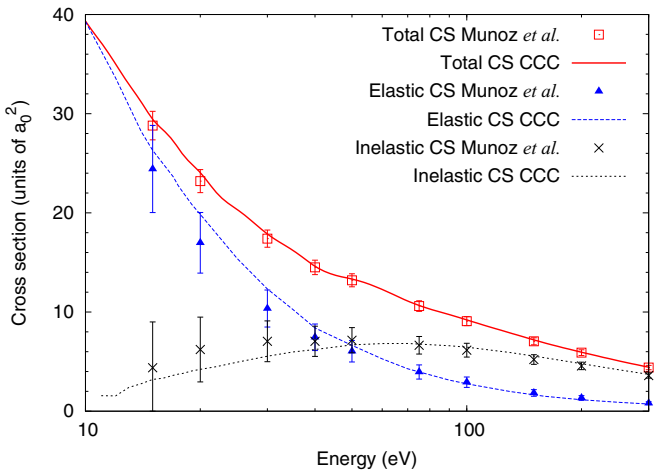

FIG. 5. Total, inelastic, and elastic cross sections (CSs) for electron scattering on the ground state of H_2. The results of the CCC calculations are compared with the cross sections adopted by Munoz *et al.* [28].

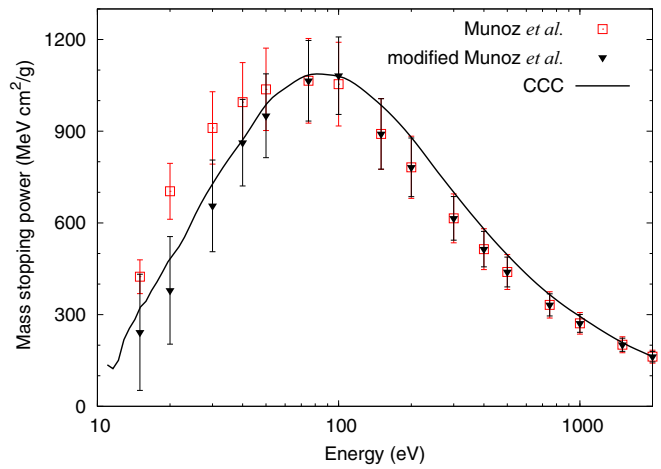

FIG. 6. Mass stopping power for electron scattering on the ground state of H_2. The CCC results are described in the text. Experimental data are due to Munoz *et al.* [28]. Modification of the absolute values and uncertainties of the experimental data of Munoz *et al.* [28] is described in the text.

the uncertainty of the present calculations due to the accuracy of the target wave functions, which we therefore estimate to be about 7%.

Given the good agreement between the CCC results and measured mean excitation energy in the 15–50 eV region, the discrepancy for the SP in this energy region should be due to the total and elastic cross sections used by Munoz *et al.* [28]. In Fig. 5 we compare total and elastic cross sections obtained in the CCC(491) calculations with the values used by Munoz *et al.* [28]. For the total cross sections we find generally better agreement than for the elastic cross sections. For the latter the discrepancy in the 15–50 eV region is manifest. From our previous studies [32], we note that our converged CCC(491) model results are in excellent agreement with other measurements [47–50] available for this energy range. Note, however, that the origin of the apparent discrepancy for the SP in Fig. 3 is ultimately not due to the values of the elastic and total scattering cross sections used by Munoz *et al.* [28], but due to the too optimistic uncertainties of the experimental data in the 15–50 eV region.

The elastic cross sections presented in Fig. 5 have been obtained from the parameter η and total cross sections presented in Table 2 of Munoz *et al.* [28]. The parameter η (the ratio of elastic to total scattering cross sections), has been fitted by Munoz *et al.* [28] to a simple function $\eta = \exp[-0.511\ln(E_i) + 1.219]$ using the semiempirical data from van Wingerden *et al.* [46] and utilized in Eq. (19) to obtain the SP. The data of van Wingerden *et al.* [46] for energies less that 100 eV are based on experimental data of Srivastava *et al.* [51]. The uncertainty in the latter measurements is 18%. The same 18% uncertainty have been applied to the Munoz *et al.* [28] elastic cross sections presented in Fig. 5. The uncertainty of the total cross sections has been estimated by Munoz *et al.* [28] to be 5%. From the total and elastic cross sections and their uncertainties one can determine the total inelastic cross section and its uncertainty. The standard error analysis gives for the absolute uncertainties

$$\Delta_{\rm inel} = \sqrt{\Delta_{\rm tot}^2 + \Delta_{\rm el}^2}. \tag{20}$$

The total inelastic cross sections as obtained from the Munoz *et al.* [28] data and its uncertainties are also presented in Fig. 5 and compared with the results of the CCC calculations. At low energies the uncertainty in the total inelastic cross section is particularly large and exceeds 100% of the experimental value at the lowest energy (15 eV). As the incident electron energy increases the absolute value of the elastic cross section drops much faster than the total cross section and the uncertainty in the latter becomes the dominant contribution to $\Delta_{\rm inel}$. The uncertainty of the SP can now be obtained from the uncertainties of the mean excitation energy and the total inelastic cross sections

$$\Delta_{\rm SP} = Q_{\rm SP}\sqrt{(\Delta_{\bar{E}}/\bar{E})^2 + (\Delta_{\rm inel}/\sigma_{\rm inel})^2}. \tag{21}$$

Given the excellent agreement between the CCC elastic cross section [32,33] and a number of elastic cross-section measurements [47–50] we have replaced the elastic cross sections used by Munoz *et al.* [28] with the CCC cross sections in the 15–100 eV energy region, assigned a 5% uncertainty to these values, and recalculated the SP utilizing the Munoz *et al.* [28] measured mean excitation energy and their estimate of the total cross section. The SP uncertainties have been obtained as described above with $\Delta_{\rm tot}/\sigma_{\rm tot} = 5\%$ and $\Delta_{\bar{E}}/\bar{E} = 9\%$ at all energies and $\Delta_{\rm el}/\sigma_{\rm el} = 5\%$ below and at 100 eV, and $\Delta_{\rm el}/\sigma_{\rm el} = 18\%$ above 100 eV. In Fig. 6 we present the comparison of the modified experimental data and the CCC calculations for the SP. As expected, the experimental uncertainties are large at energies less than 50 eV and the CCC results are now within the error bars.

IV. CONCLUSIONS

The electron mass SP in H_2 has been calculated using the CCC method. The convergence of the SP has been established by increasing the size of the close-coupling expansion from 9 to 491 states. The ionization channels have been found to make major contributions to the SP. We

estimate that the uncertainties of the CCC SP and mean excitation energy are better than 9%, which is due to the convergence of the close-coupling expansion (5%) and the underlying target structure accuracy (7%). The accuracy of the present CCC results is a significant improvement over previous SP estimates produced from available experimental e^--H_2 cross sections and Born-Bethe theory [17,25–27]. We find generally reasonably good agreement with these estimates of the SP, in particular with the data of Dalgarno *et al.* [17]. Good agreement with measurements of Munoz *et al.* [28] is found over the energy range 15–2000 eV, though an apparent discrepancy in the 15–50 eV region was identified. We determined that this discrepancy is due to the too optimistic experimental uncertainties in this energy region. Comparison with the directly measured mean excitation energy showed excellent agreement in the same energy region. We have confirmed for H_2 that the procedure used by Munoz *et al.* [28] to calculate the SP is sufficiently reliable when accurate elastic and total cross sections are used, however, it can lead to large experimental uncertainties for incident electron energies up to few times the ionization potential.

ACKNOWLEDGMENTS

We would like to thank Dr. J. Colgan for reviewing this manuscript. This work was supported by the United States Air Force Office of Scientific Research, Los Alamos National Laboratory (LANL) and Curtin University. M.C.Z. would like to specifically acknowledge LANL's ASC PEM Atomic Physics Project for its support. The LANL is operated by Los Alamos National Security, LLC for the National Nuclear Security Administration of the U.S. Department of Energy under Contract No. DE-AC52- 06NA25396. Resources were provided by the Pawsey Supercomputing center with funding from the Australian government and the government of Western Australia.

[1] B. Boudaïffa, P. Cloutier, D. Hunting, M. A. Huels, and L. Sanche, Science **287**, 1658 (2000).
[2] X. Pan, P. Cloutier, D. Hunting, and L. Sanche, Phys. Rev. Lett. **90**, 208102 (2003).
[3] L. Campbell and M. Brunger, Int. Rev. in Phys. Chem. **35**, 297 (2016).
[4] M. Padovani, D. Galli, and A. E. Glassgold, A&A **501**, 619 (2009).
[5] *Atomic and Molecular Processes in Fusion Edge Plasmas*, edited by R. K. Janev (Plenum, New York, 1995).
[6] I. Bray, D. V. Fursa, A. S. Kheifets, and A. T. Stelbovics, J. Phys. B: At. Mol. Opt. Phys. **35**, R117 (2002).
[7] O. Zatsarinny and K. Bartschat, J. Phys. B: At. Mol. Opt. Phys. **46**, 112001 (2013).
[8] J. Colgan, M. S. Pindzola, F. J. Robicheaux, D. C. Griffin, and M. Baertschy, Phys. Rev. A **65**, 042721 (2002).
[9] J. Carr, P. Galiatsatos, J. Gorfinkiel, A. Harvey, M. Lysaght, D. Madden, Z. Masin, M. Plummer, J. Tennyson, and H. Varambhia, Eur. Phys. J. D **66**, 1 (2012).
[10] R. F. da Costa, M. T. do N. Varella, M. H. F. Bettega, and M. A. P. Lima, Eur. Phys. J. D **69**, 159 (2015).
[11] P. Mayles, A. Nahum, and J. C. Rosenwald, *Handbook of Radiotherapy Physics: Theory and Practice* (CRC Press, Boca Raton, 2007).
[12] B. J. MvParland, *Nuclear Medicine Radiation Dosimetry : Advanced Theoretical Principles* (Springer, Berlin, 2010).
[13] M. Kimura, M. Inokuti, and M. A. Dillon, Adv. Chem. Phys. **84**, 193 (1993).
[14] R. B. Miller, *Electronic irradiation of foods: introduction to the technology* (Springer, Berlin, 2005).
[15] J. L. Fox, M. I. Galand, and R. E. Johnson, Space Sci. Rev. **139**, 3 (2008).
[16] Y. Xu and R. McCray, Astrophys. J. **375**, 190 (1991).
[17] A. Dalgarno, M. Yan, and W. Liu, Astrophys. J. Suppl. **125**, 237 (1999).
[18] F. Rohrlich and B. C. Carlson, Phys. Rev. **93**, 38 (1954).
[19] M. Inokuti, Rev. Mod. Phys. **43**, 297 (1971).
[20] International Commission on Radiation Units and Measurements, ICRU Report No. 37, 1984.
[21] W. Bragg and R. Kleeman, Philos. Mag. **10**, 318 (1905).
[22] M. J. Berger, J. S. Coursey, M. A. Zucker, and J. Chang, NIST standard reference database 124, 2005, URL http://physics.nist.gov/PhysRefData/Star/Text/method.htm.
[23] I. Maglevanny, V. Smolar, and H. Nguyen, Nucl. Instr. and Meth. B **316**, 123 (2013).
[24] H. Sugiyama, Phys. Med. Biol. **30**, 331 (1985).
[25] H. Gumus, Radiat. Phys. Chem. **72**, 7 (2005).
[26] K. Takayanagi and K. Nakata, Bull. Inst. Space Aeronaut. Sci. **6**, 849 (1970).
[27] W. T. Miles, R. Thompson, and A. E. S. Green, J. Appl. Phys. **43**, 678 (1972).
[28] A. Munoz, J. C. Oller, F. Blanco, J. D. Gorfinkiel, and G. García, Chem. Phys. Lett. **433**, 253 (2007).
[29] J. C. Oller, A. Munoz, J. M. Pérez, F. Blanco, P. Limao-Vieira, and G. García, Chem. Phys. Lett. **421**, 439 (2006).
[30] G. García and F. Blanco, Phys. Lett. A **279**, 61 (2001).
[31] F. Blanco and G. García, Phys. Lett. A **317**, 458 (2003).
[32] M. C. Zammit, J. S. Savage, D. V. Fursa, and I. Bray, Phys. Rev. Lett. **116**, 233201 (2016).
[33] M. C. Zammit, J. S. Savage, D. V. Fursa, and I. Bray, Phys. Rev. A **95**, 022708 (2017).
[34] J. J. Bailey, A. S. Kadyrov, I. B. Abdurakhmanov, D. V. Fursa, and I. Bray, Phys. Rev. A **92**, 022707 (2015).
[35] J. J. Bailey, A. S. Kadyrov, I. B. Abdurakhmanov, D. V. Fursa, and I. Bray, Phys. Rev. A **92**, 052711 (2015).
[36] M. C. Zammit, D. V. Fursa, J. S. Savage, and I. Bray, J. Phys. B: At. Mol. Opt. Phys. **50**, 123001 (2017).
[37] M. C. Zammit, D. V. Fursa, and I. Bray, Phys. Rev. A **90**, 022711 (2014).
[38] I. Bray and A. T. Stelbovics, Phys. Rev. A **46**, 6995 (1992).
[39] K. Bartschat, E. T. Hudson, M. P. Scott, P. G. Burke, and V. M. Burke, J. Phys. B: At. Mol. Opt. Phys. **29**, 115 (1996).
[40] J. D. Gorfinkiel and J. Tennyson, J. Phys. B: At. Mol. Opt. Phys. **38**, 1607 (2005).

[41] M. C. Zammit, D. V. Fursa, J. S. Savage, I. Bray, L. Chiari, A. Zecca, and M. J. Brunger, Phys. Rev. A **95**, 022707 (2017).
[42] S. E. Branchett, J. Tennyson, and L. A. Morgan, J. Phys. B: At. Mol. Opt. Phys. **23**, 4625 (1990).
[43] S. E. Branchett, J. Tennyson, and L. A. Morgan, J. Phys. B: At. Mol. Opt. Phys. **24**, 3479 (1991).
[44] R. F. da Costa, F. J. da Paixão, and M. A. P. Lima, J. Phys. B: At. Mol. Opt. Phys. **38**, 4363 (2005).
[45] I. Bray, Phys. Rev. Lett. **73**, 1088 (1994).
[46] B. van Wingerden, R. W. Wagenaar, and F. J. de Heer, J. Phys. B: At. Mol. Opt. Phys. **13**, 3481 (1980).
[47] T. W. Shyn and W. E. Sharp, Phys. Rev. A **24**, 1734 (1981).
[48] H. Nishimura, A. Danjo, and H. Sugahara, J. Phys. Soc. Jpn. **54**, 1757 (1985).
[49] M. A. Khakoo and S. Trajmar, Phys. Rev. A **34**, 138 (1986).
[50] J. Muse, H. Silva, M. C. A. Lopes, and M. A. Khakoo, J. Phys. B: At. Mol. Opt. Phys. **41**, 095203 (2008).
[51] S. K. Srivastava, A. Chutjian, and S. Trajmar, J. Chem. Phys. **63**, 2659 (1975).